IEEE Access
Multidisciplinary | Rapid Review | Open Access Journal

Received 2 April 2023, accepted 10 April 2023, date of publication 14 April 2023, date of current version 21 April 2023.

Digital Object Identifier 10.1109/ACCESS.2023.3267410

RESEARCH ARTICLE

An Energy Management System for the Optimal Operation of BESS in DC Microgrids: A Robust Convex Programming Approach

WALTER GIL-GONZÁLEZ[1], (Member, IEEE), OSCAR DANILO MONTOYA[2], (Member, IEEE), AND JESÚS C. HERNÁNDEZ[3]

[1]Department of Electrical Engineering, Universidad Tecnológica de Pereira, Pereira 660003, Colombia
[2]Facultad de Ingeniería, Universidad Distrital Francisco José de Caldas, Bogotá, Distrito Capita 110231, Colombia
[3]Department of Electrical Engineering, University of Jaén, 23071 Jaén, Spain

Corresponding authors: Oscar Danilo Montoya (odmontoyag@udistrital.edu.co) and Jesús C. Hernández (jcasa@ujaen.es)

This work was supported in part by the Council of Andalucía (Junta de Andalucía, Consejería de Transformación Económica, Industria, Conocimiento y Universidades, Secretaría General de Universidades, Investigación y Tecnología) through Project ProyExcel_0038.

ABSTRACT This paper uses a convex reformulation to deal with the robust, optimal energy management of battery energy storage systems (BESS) and renewable energies in DC microgrids. This relaxed mathematical model guarantees the global optimum regarding energy management problems, even when including uncertainties in demand and renewable energy. The proposed robust model can reach the best scheduling for energy management in worst-case cost scenarios while satisfying all requirements. Furthermore, a model for power transfer losses in converter devices is added to the proposed model by using a binary polynomial representation, which is convexified. This convexification is performed by transforming the nonlinear non-convex equations of the optimal energy management model into second-order cone constraints. Four scenarios implemented in the modified IEEE 123-bus radial distribution feeder are proposed in order to analyze the robust optimal energy management strategy: the deterministic model, demand uncertainty, uncertainty in solar and wind generators, and uncertainty in demand and solar and wind generators. In all scenarios, the energy management model reduces the total energy costs. Simulation scenario 1 showed daily operating costs of about US$ 4376.82, while simulation scenarios 2, 3, and 4, including demand and generation uncertainties, increased the daily operating costs by about US$ 5243.23 (19.79%), US$ 5072.23 (15.88%), and US$ 5738.75 (31.12%), respectively. Scenario 4 showed the highest costs, as it involves more uncertainty. Hence, the robust optimal energy management strategy dispatches more energy from conventional generators, increasing the operating costs to satisfy those of the worst case.

INDEX TERMS Battery energy storage systems, energy management optimal, mixed-integer robust convex model, power transfer losses.

NOMENCLATURE

ACRONYMS

AC	Alternating current.
BESS	Battery energy storage system.
DC-MG	Direct current microgrid.
EMS	Energy management system.
MINLP	Mixed-integer nonlinear programming.
PV	Photovoltaic.
SoC	State of charge (BESS).

The associate editor coordinating the review of this manuscript and approving it for publication was Giambattista Gruosso.

PARAMETERS

Δt	Duration of a single time period (s).
$\hat{d}_k^t$	Deviation by renewable generation (or demand) from its nominal value at node k and time t. (W).
ϕ^k	Charging efficiency of the BESS connected to node k (1/W).
$C^{k,t}$	Conventional generator power purchase costs at node k and time t ($/kWh).
c_{a0}	Independent coeff icient of the AC-DC converter polynomial loss model (W).
c_{a1}	Linear coefficient of the AC-DC converter polynomial loss model.

c_{a2} Quadratic coefficient of the AC-DC converter polynomial loss model (1/W).
c_{b0} Independent coefficient of the battery polynomial loss model (W).
c_{b1} Quadratic coefficient of the battery polynomial loss model (1/W).
c_{d0} Independent coefficient of the DC-DC converter polynomial loss model (W).
c_{d1} Linear coefficient of the DC-DC converter polynomial loss model.
c_{d2} Quadratic coefficient of the DC-DC converter polynomial loss model (1/W).
p_t Day-ahead market price at time t ($/kWh).
p_{max_l} Maximum power flow in branch l (W).
$p^k_{min_b}, p^k_{max_b}$ Minimum and maximum power capacity of the BESS at node k (W).
$p^k_{min_{gen}}, p^k_{max_{gen}}$ Minimum and maximum power capacity of the conventional generators at node k (W).
$p^k_{min_{ren}}, p^k_{max_{ren}}$ Minimum and maximum power capacity of the renewable energy generators at node k (W).
SoC^k_f Final SoC of the BESS at node k.
SoC^k_t Initial SoC of the BESS at node k.
$u^{0,t}$ Squared voltage at the slack node at time t (V^2).
u_{min}, u_{max} Minimum and maximum limits regarding squared voltage ($u_{min} = (v_{min})^2$, $u_{max} = (v_{max})^2$) (V^2).

SETS AND INDICES

Ω_b Set of network branches.
Ω_n Set of network nodes.
Ω_t Set of network time periods.
D^t Uncertainty set of nodes at time t.
$k,\ m$ Node indices ($k, m \in \Omega_n$).
l Branch indices km ($km \in \Omega_b$).
t Time indices.

VARIABLES

$p^{k,t}_{gen}$ Power provided by the conventional generator at node k and time t (W).
$P^{k,t}_{loss_b}$ Power losses of the battery at node k and time t (W).
$P^{k,t}_{loss_{conv}}$ Power losses of the converter at node k and time t (W).
$\theta^{k,t}_+,\ \theta^{k,t}_-$ Binary variable used to define the uncertainty at node k and time t.
k Auxiliary variable for the converter (W^2).
$k^{k,t}$ Auxiliary variable for the converter at node k and time t (W^2).
$k^{k,t}_b$ Auxiliary variable for the battery at node k and time t (W^2).
k_b Auxiliary variable for the battery (W^2).
$p_{AC-loss_{conv}} v^{k,t}$ Power losses of the AC-DC converter at node k and time t (W).
$p^{k,t}_{bess}$ Power provided by the BESS at node k and time t (W).
$p^{k,t}_b$ Power provided by the battery at node k and at time t (W).
$p^{k,t}_{DC-loss_{conv}}$ Power losses of the DC-DC converter at node k and time t (W).
P_{loss_b} Power losses of the battery at time t (W).
$P^{k,t}_{loss_{conv}}$ Power losses of the converter at node k and time t (W).
$p^{r,t}_l$ Receiving power flow in branch l at time t (W).
$p^{s,t}_l$ Sending power flow in branch l at time t (W).
$p^{k,t}_{PV}$ Power injected by the PV system at node k and time t (W).
$p^{k,t}_{pv}$ Power injected by the solar panels at node k and time t (W).
$p^{k,t}_{ren}$ Power provided by the renewable energy generator at node k and time t (W).
$p^{k,t}_{WIND}$ Power injected by the wind power system at node k and time t (W).
$p^{k,t}_{wind}$ Power generated by the wind generator at node k and time t (W).
s_t Binary variable that defines the operation state of the converter at time t.
SoC^k_t State of charge of BESS at node k and time t.
$u^{k,t}$ Squared voltage at node k and time t (V^2).
$v^{k,t}$ Voltage at node k and time t (V).
$w^{l,t}$ Voltage product ($v^{k,t} \times v^{m,t}$) in branch l at time t (V^2).

I. INTRODUCTION

The continuing need to diversify the energy matrix has sparked the study and development of new technologies such as renewable energy (solar, wind, geothermal, bio-energy, among others) and energy storage (batteries, superconducting magnetic, and flywheels, among others) [1], [2]. These technologies have the attention of the global energy transition because of their significant advantages, such as lower emissions by fossil fuels, cleaner air and water, and cheaper ways to generate electricity, among others [3]. However, they have some disadvantages, such as their dependency on environmental conditions, higher capital costs than conventional technologies, and the challenging management of energy storage systems, among others. Despite all of the above, new technologies continue to emerge in the energy development path [4], [5]. Therefore, facing all challenges from the perspective of control and energy management strategies has been a challenge for multiple researchers.

On the other hand, DC microgrids have proven to be more attractive than their AC counterpart, as they have several advantages, including lower losses, higher efficiency, a more straightforward connection, excellent reliability, and simpler control schemes (no control frequency and reactive power required) [6]. Furthermore, they allow for a direct connection between renewable energy sources, energy storage systems, and electronic DC loads, reducing investment costs and energy conversion stages [7]. Even with all these advantages, the DC microgrids still require good coordination and interaction between the systems comprising it in order to guarantee optimal resource management and enhance power quality [8], [9]. Energy storage systems, such as battery energy storage systems (BESS), help maintain better coordination and interaction in DC microgrids, as they can respond quickly, require small spaces and little time for installation, and reduce pollution [10], [11]. They can also alleviate the load curve by delivering power during energy shortages and absorbing power during abundance periods [12], [13].

The design of energy management systems (EMS) for microgrids is a complex task from an optimization perspective, given that the following criteria must be met:

i. An objective function indicator must be minimized, which can be technical, economic, or environmental.
ii. Optimal power injection in the renewable energy resources and the BESS charging/discharging profiles must be determined.
iii. The efficient solution of the exact mixed-integer nonlinear programming (MINLP) model must represent the studied problem, with the main complication of coupling in the time variable.

Multiple works have been proposed in the specialized literature to address the complexities of designing an efficient EMS for renewables and BESS in microgrids. Some of these recent advances are discussed below. The authors of [14] presented a grid-scale design for a BESS in the context of the Colombian electricity market. The authors showed a design of the BESS that considered the battery's lifespan and its operating characteristics regarding the state of charge and deep discharge. A mixed-integer linear programming model was used to determine the optimal operation of the BESS by predicting the price and demand with historical data. Numerical results showed that additional analysis is required regarding economic incentives to make the integration of BESS systems economically viable in the Colombian electricity market. The work by [15] presented the optimal integration and operation of BESS and renewables in distribution networks, considering an MINLP formulation. In the first stage, the optimal location of the BESS and renewable generators was determined by applying a metaheuristic method based on simulated annealing to select the nodes where these devices must be located. In the second stage, an optimization model based on mixed-integer convex programming was implemented to define the optimal size and operation of the distributed energy resources, with the aim of minimizing the expected annual investment and operating costs. Numerical results in test feeders with 11 to 230 nodes demonstrated the effectiveness of the proposed optimization model when compared to linear approximations and conic programming methods. In [16], a semi-definite programming formulation of the problem regarding the efficient operation of BESS in monopolar DC networks was proposed. The exact nonlinear programming model was regulated using the semi-definite representation of the product between the voltage variables of all network nodes, which allowed transforming it into a convex approximated model. Numerical results in the 21-bus grid demonstrated the effectiveness of the convex approach in comparison with the exact nonlinear programming solution in the GAMS software [17]. The authors of [18] presented a mixed-integer linear programming formulation to solve the problem regarding the optimal placement and sizing of renewable generators based on photovoltaic (PV) sources and BESS in distribution networks while considering the loadability of the upstream transformer. Numerical results demonstrated that, with adequate scheduling of the distributed energy resources, the energy transference capability of the distribution network could be increased to 1.7 times that of the benchmark case (without BESS and PV sources), which would allow supplying energy to new users with the same electrical infrastructure. In [19], the application of a master-slave optimization approach based on the parallel version of the particle swarm optimizer and the successive approximations power flow method was proposed to define the optimal operation of BESS in DC microgrids. Numerical results in the 21-bus grid demonstrated the effectiveness of the proposed approach when compared to the black hole optimizer and genetic algorithms. The study by [20] presented a convex approximation to design an efficient EMS system for BESS and PV sources in monopolar DC networks. The authors used the McCormick approximation to relax the power balance constraint in order to obtain a recursive quadratic convex model. The minimization of the daily energy losses was considered as an objective function. Numerical results in the DC version of the IEEE 33-bus grid showed the effectiveness of the proposed EMS when compared to different combinatorial optimizers, *i.e.*, the particle swarm optimizer, the salp swarm algorithm, the multi-verse optimizer, and the crow search algorithm. In the work by [21], a day-ahead analysis was conducted via a linear programming model to determine the periods in which the BESS can be dispatched to reduce the peak of load consumptions. Once the periods when the BESS must be operated had been determined, a real-time control approach was implemented in order to define the discharging profile of the BESS, with the purpose of minimizing the total grid energy purchasing costs, which was based on a variable tariff methodology. The proposed EMS found reductions of about 12% in the expected grid operating costs.

In light of the above, two main aspects are identified: (i) Most of the authors in the above-presented literature review neglect the effect of energy losses on the power electronic converters that interface the BESS and

renewable energy resources, which allows simplifying the exact MINLP models that define the operation of the batteries into mixed-integer linear programming or nonlinear (continuous) programming models; and (ii) the stochastic nature of renewable generation and demand profiles are not considered. These two aspects allow this research to make the following contributions:

i. A mixed-integer robust convex model for the optimal scheduling of EMS in a DC microgrid is described. The proposed robust model is solved in two adaptive stages, as proposed in [22]. The first stage computes the variables associated with energy management optimization scheduling, which considers the worst-case uncertainty in demand and renewable energy generation; while the second stage determines the uncertainties in certain ranges.
ii. A power transfer losses model for converter devices is included in the optimal convex model using the binary-polynomial constraint presented in [23]. This model is relaxed, employs a second-order cone constraint, and allows considering power transfer losses in each converter to correctly compute the optimal EMS scheduling in the DC microgrid.
iii. Several proposed scenarios in the modified IEEE 123-bus radial distribution feeder demonstrate that the robust convex model can optimally schedule the EMS while considering uncertainty in demand and solar and wind generators.

It is essential to mention that the binary-polynomial constraints for the power transfer losses model for converter devices have also been included in [23]. However, this study focused on the optimal programming of the plug-in and plug-off of the energy storage devices in two AC distribution networks, with the aim to maximize the devices' value in several scenarios. This optimal programming also used robust optimization.

On the other hand, within the scope of this research, it is assumed that the distribution company has already established the nodes for the distributed energy resources (*i.e.*, BESS and renewable energy resources) and their sizes. This implies that the main interest of this research is proposing an efficient EMS system to operate/manage distributed energy resources in the DC microgrid (DC-MG) under analysis.

The remainder of this document is organized as follows. Section II models the power transfer losses in converter devices as binary-polynomial constraints, which are transformed into second-order cone constraints. Section III describes the energy management model for optimally scheduling BESS and renewable energy sources in DC microgrids. This section also presents the deterministic and robust optimization models. Section IV shows the test system, proposed scenarios, and results. Finally, the main conclusions are drawn in Section V.

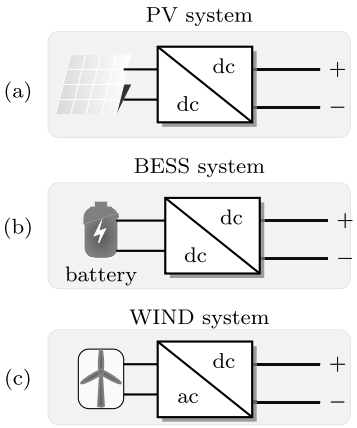

FIGURE 1. Schematic of renewable energy and BESS integration: (a) PV generator connects to the DC-MG via a DC-DC converter, (b) BESS connects to the DC-MG via a DC-DC converter, and (c) wind generator connects to the DC-MG via an AC-DC converter.

II. POWER TRANSFER LOSSES MODEL IN DEVICES

Models for renewable energy and BESS integration are usually constructed through power electronic converter devices. Usually, these devices are modeled without considering their power losses, which can lead to an error in the optimal energy management of a DC microgrid. Therefore, the result obtained may not be the optimal system. Fig. 1 illustrates the typical integration of these systems, where PV power generation and BESS are integrated through a DC-DC converter. In contrast, wind power generation is integrated via an AC-DC converter.

The power losses in the AC-DC and DC-DC converters are represented by combining a binary variable and the quadratic polynomial of the active power [23], [24], as follows:

$$P_{loss_{conv}} = s(c_0 + c_1 P + c_2 P^2), \tag{1}$$

where s corresponds to the state of the converter ($s = 1$ if the converter is energized and $s = 0$ if the converter is de-energized); P represents the active power flow between the systems and the DC-MG; the coefficients c_0, c_1, and c_2 represent the different types of losses within a converter [25], [26]; c_0 corresponds to no-load energization losses associated with the converter's passive components (filters and transformer); and the coefficients c_1 and c_2 correspond to switching and power conduction losses in the converter [27].

On the other hand, the battery losses P_{loss_b} can be modeled as follows:

$$P_{loss_b} = c_{b_0} + c_{b_1} P_b^2, \tag{2}$$

where P_b is the power of the battery; the coefficient c_{b_0} is an auxiliary variable that represents the system losses in the battery, and the coefficient c_{b_1} represents the power losses in the battery due to its internal resistance. Note that, in the batteries, there are losses given by c_{b_0}, even though there is no load, which is due to the chemical processes taking place in them [28].

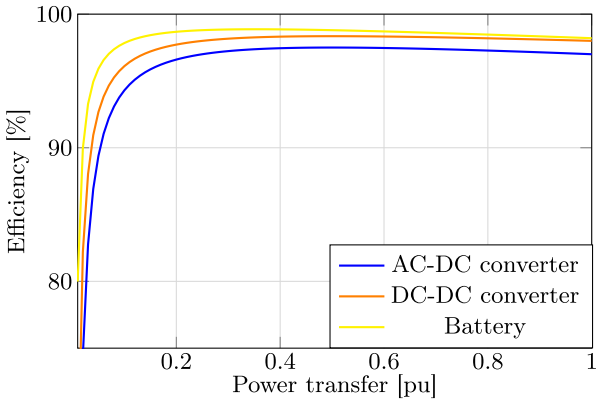

FIGURE 2. Efficiency for the AC-DC converter, the DC-DC converter, and the battery as a power transfer function.

TABLE 1. Coefficient values for losses in the devices.

Device	AC-DC converter			DC-DC converter			Battery	
Coefficient	c_{a0}	c_{a1}	c_{a2}	c_{d0}	c_{d1}	c_{d2}	c_{b0}	c_{b1}
Value	0.5	0.5	2.0	0.35	0.25	1.4	0.2	1.6

Fig. 2 depicts the efficiencies of the AC-DC and DC-DC converters and batteries *vs.* their chargeability. The curves shown in this figure are elaborated with the coefficients listed in Table 1, which are taken from [23].

Note that the power losses in the AC-DC and DC-DC converters are non-linear, non-convex equations. Therefore, it is necessary to express these equations in convex form to ensure a global optimal solution to the problem. The power losses in the AC-DC and DC-DC converters (1) can be represented as a linear constraint, as follows:

$$P_{loss_{conv}} = sc_0 + c_1 P_{abs} + c_2\, k, \tag{3}$$

where

$$P_{abs} = |P|, \tag{4}$$
$$k = P^2. \tag{5}$$

The constraint (4) can be easily transformed into a linear constraint:

$$-P \le P_{abs} \le P. \tag{6}$$

The constraint (5) can be rewritten using a second-order cone constraint representation, as follows:

$$\begin{aligned} P^2 = \|P\|^2 =& k = \frac{1}{4}(k+1)^2 - \frac{1}{4}(1-k)^2 \\ (1-k)^2 + \|2P\|^2 =& (k+1)^2 \\ \left\| \begin{matrix} 2P \\ 1-k \end{matrix} \right\| =& k+1. \end{aligned} \tag{7}$$

This second-order cone constraint remains non-convex. Hence, the equality is relaxed in order to transform it into a convex constraint, namely

$$\left\| \begin{matrix} 2P \\ 1-k \end{matrix} \right\| \le k+1. \tag{8}$$

Similarly, a process can be performed to transform the battery losses (2) into a linear constraint:

$$P_{loss_b} = c_{b0} + c_{b1} k_b, \tag{9}$$

with

$$k_b = P_b^2, \tag{10}$$

which can also be relaxed into a second-order cone constraint by following the same procedure for the converter power losses. Finally, the second-order cone constraint for the constraint (10) is

$$\left\| \begin{matrix} 2P_b \\ k_b - 1 \end{matrix} \right\| \le k_b + 1. \tag{11}$$

III. ENERGY MANAGEMENT MODEL

The optimal energy management problem for BESS deals with minimizing the total energy costs in a DC-MG. The formulation of this problem is presented in this section, which is divided into the objective function, the constraints, and the entire model.

A. OBJECTIVE FUNCTION

The objective function for the optimal energy management of BESS in DC-MGs corresponds to the minimization of the total energy costs. A single objective function (in monetary terms) is considered in this paper, which contains the cost of power transfer losses $f_{cost}^{device-losses}$ (*i.e.*, AC-DC converter for wind power, DC-DC converter for solar power and the BESS, and the battery), the cost of network losses $f_{cost}^{grid-losses}$, and the cost of the energy from conventional generation f_{cost}^{gen}. The objective function is described below:

$$\min f = f_{cost}^{device-losses} + f_{cost}^{gen} + f_{cost}^{grid-losses}, \tag{12}$$

with

$$f_{cost}^{device-losses} = \sum_{t\in\Omega_t} \left(P_{loss_{conv}}^{k,t} + P_{loss_b}^{k,t} \right) p_t \Delta t, \tag{13}$$
$$f_{cost}^{gen} = \sum_{t\in\Omega_t} C^{k,t} p_{gen}^{k,t} \Delta t, \tag{14}$$
$$f_{cost}^{grid-losses} = \sum_{t\in\Omega_t} \sum_{l\in\Omega_b} \left(p_l^{s,t} + p_l^{r,t} \right) p_t \Delta t, \tag{15}$$

B. CONSTRAINTS OF THE ENERGY MANAGEMENT MODEL

1) POWER FLOW BALANCE

The power flow balance generates a set of constraints given by the power flow in the branch, as well as the by power generated and the demand in the nodes, which must satisfy the energy balance. Fig. 3 illustrates an example of a generic branch $l = (km) \in \Omega_b$ at time $t \in \Omega_t$.

Note that the power flowing from k to m ($p_l^{s,t}$) is called the *sending power flow*, while the power flowing from m to k ($p_l^{r,t}$) is the *receiving power flow*. These power flows are different ($p_l^{s,t} \neq p_l^{r,t}$) and given by

$$p_l^{s,t} = v^{k,t} y_l \left(v^{k,t} - v^{m,t} \right), \tag{16}$$

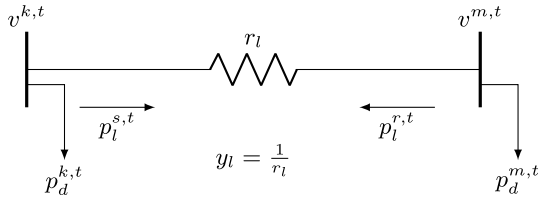

FIGURE 3. Example of a generic branch in a DC-MG.

$$p_l^{r,t} = v^{m,t} y_l \left(v^{m,t} - v^{k,t}\right). \tag{17}$$

The power flow loss in the branch l is computed as the sum of the sending and receiving power flows in the branch, as follows:

$$\begin{aligned} p_{loss_l}^t &= p_l^{s,t} + p_l^{r,t} = \\ &= y_l \left(\left(v^{k,t}\right)^2 - 2v^{k,t}v^{m,t} + \left(v^{m,t}\right)^2 \right). \end{aligned} \tag{18}$$

Note that the power flow constraints (16) and (17) and the power flow losses (19) are non-linear and non-convex, indicating that a global optimum cannot be achieved in the overall problem and its solution is difficult. However, it is possible to transform them into linear constraints by defining the following two auxiliary variables:

$$u^{k,t} = \left(v^{k,t}\right)^2, \tag{19}$$

$$w^{l,t} = v^{k,t} v^{m,t}. \tag{20}$$

Now, by substituting these auxiliary variables in (16) and (17) and the power flow losses (19), the following is obtained:

$$p_l^{s,t} = y_l \left(u^{k,t} - w^{l,t}\right), \tag{21}$$

$$p_l^{r,t} = y_l \left(u^{m,t} - w^{l,t}\right), \tag{22}$$

$$p_{loss_l}^t = y_l \left(u^{k,t} - 2w^{l,t} + u^{m,t}\right). \tag{23}$$

Even though the above-presented constraints are already linear, the auxiliary variables must still be transformed into a second-order cone constraint, with the aim to generate a non-convex model defined as

$$\begin{aligned} w^{l,t} &= v^{k,t} v^{m,t} \\ w^{l,t} w^{l,t} &= \left(v^{k,t}\right)^2 \left(v^{m,t}\right)^2 \\ \left\| w^{l,t} \right\|^2 &= u^{k,t} u^{m,t} \\ \left\| \begin{matrix} 2w^{l,t} \\ u^{k,t} - u^{m,t} \end{matrix} \right\| &= u^{k,t} + u^{m,t} \\ \left\| \begin{matrix} 2w^{l,t} \\ u^{k,t} - u^{m,t} \end{matrix} \right\| &\leq u^{k,t} + u^{m,t}. \end{aligned} \tag{24}$$

Fig. 4 presents the graphical representation of the power flow equations. The constraint that represents the power flow balance at node k and time t is given by

$$p_{gen}^{k,t} + p_{ren}^{k,t} + p_{bess}^{k,t} - p_d^{k,t} = \sum_{l \in L} \left(A_{kl}^+ p_l^{s,t} + A_{kl}^- s_l^{r,t}\right), \tag{25}$$

where $A = A^+ + A^-$ is the incidence matrix, with A^+ containing the positive values and A^- the negative ones.

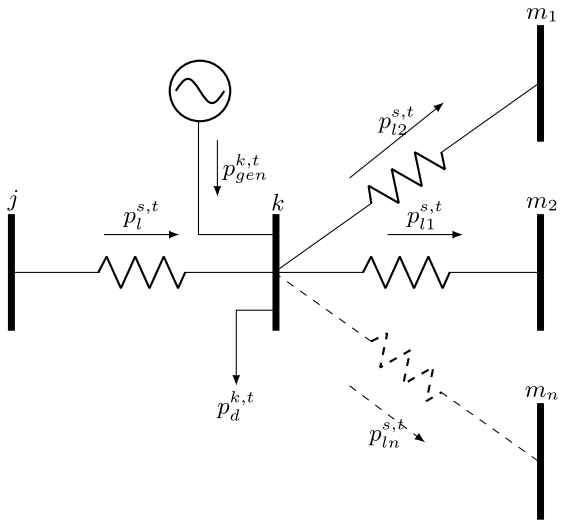

FIGURE 4. Graphical representation of the power flow equations in a DC-MG.

2) BESS OPERATION

The battery operation is ruled by its state of charge (SoC), which varies as a function of the power absorbed or injected by the DC-MG plus its losses, as follows:

$$SoC_{t+1}^k = SoC_t^k - \phi^k (p_b^{k,t} + p_{loss_b}^{k,t}), \tag{26}$$

$$SoC_{t=1}^k = SoC_0^k, \tag{27}$$

$$SoC_{t=T}^k = SoC_f^k. \tag{28}$$

The SoC of each battery has capacity limits for stored energy (*i.e.*, between 0 and 100%). There are also limits regarding power transfer in the BESS, which is related to its minimum and maximum capacity. Hence, these limits must also be considered as constraints, as follows:

$$0 \leq SoC_t^k \leq 1, \tag{29}$$

$$p_{min_b}^k \leq p_b^{k,t} \leq p_{max_b}^k. \tag{30}$$

It is important to highlight that the useful life of the BESS depends directly on its storage limits, which can be increased if lower limits are considered, as recommended by the IEEE 1561-2007 standard [29].

The whole power absorbed or injected by the BESS comprises battery power and losses and DC-DC converter losses:

$$p_{bess}^{k,t} = p_b^{k,t} + p_{loss_b}^{k,t} + p_{DC-loss_{conv}}^{k,t}, \tag{31}$$

$$-p_{max_{DC-conv}}^k \leq p_{DC-loss_{conv}}^{k,t} \leq p_{max_{DC-conv}}^k, \tag{32}$$

where $p_{DC-loss_{conv}}^{k,t}$ denotes the power losses of the DC-DC converter at node k and time t.

3) GENERATOR OPERATION

A DC-MG includes conventional and renewable energy generators. Only the minimum and maximum limits of the conventional generators' capacity are considered, as follows:

$$-p_{min_{gen}}^k \leq p_{gen}^{k,t} \leq p_{max_{gen}}^k. \tag{33}$$

On the other hand, renewable energy generators are integrated into the DC-MG through power electronic converters. If these generators are based on solar energy, they are connected to the grid via DC-DC converters, whereas those based on wind energy are integrated through AC-DC converters. Therefore, the injected power of these generators must include the power losses in the converters. Hence, their power is defined as

$$p_{PV}^{k,t} = p_{pv}^{k,t} + p_{DC-loss_{conv}}^{k,t}, \tag{34}$$
$$p_{WIND}^{k,t} = p_{wind}^{k,t} + p_{AC-loss_{conv}}^{k,t}, \tag{35}$$

whose limits are

$$p_{min_{ren}}^{k} \leq p_{PV}^{k,t} \leq p_{max_{ren}}^{k}, \tag{36}$$
$$p_{min_{ren}}^{k} \leq p_{WIND}^{k,t} \leq p_{max_{ren}}^{k}, \tag{37}$$
$$-p_{max_{AC-conv}}^{k} \leq p_{AC-loss_{conv}}^{k,t} \leq p_{max_{AC-conv}}^{k}. \tag{38}$$

4) OPERATING LIMITS OF THE DC-MG

The operating limits of a DC-MG are given by the nodal voltages and the power flow capacity of the lines.

$$u_{min} \leq u^{k,t} \leq u_{max}, \tag{39}$$
$$-p_{max_l} \leq p_l^{s,t} \leq p_{max_l}, \tag{40}$$
$$-p_{max_l} \leq p_l^{r,t} \leq p_{max_l}, \tag{41}$$

where u_{min} and u_{max} are limits regarding the minimum and maximum squared voltage.

5) ENERGY MANAGEMENT OPTIMIZATION MODEL

The convex representation of the full energy management optimization model is shown below:

$$\min f_{cost}^{device-losses} + f_{cost}^{gen} + f_{cost}^{grid-losses}$$

subject to

$$p_{gen}^{k,t} + p_{ren}^{k,t} + p_{bess}^{k,t} - p_d^{k,t} = \sum_{l \in L} \left(A_{kl}^{+} p_l^{s,t} + A_{kl}^{-} s_l^{r,t} \right)$$
$$p_l^{s,t} = y_l \left(u^{k,t} - w^{l,t} \right)$$
$$p_l^{r,t} = y_l \left(u^{m,t} - w^{l,t} \right)$$
$$u^{0,t} = \left(v^{\text{nom}} \right)^2$$
$$\left\| \begin{matrix} 2w^{l,t} \\ u^{k,t} - u^{m,t} \end{matrix} \right\| \leq u^{k,t} + u^{m,t}$$
$$\left\| \begin{matrix} 2P \\ k^{k,t} - 1 \end{matrix} \right\| \leq k^{k,t} + 1$$
$$\left\| \begin{matrix} 2p_b^{k,t} \\ k_b^{k,t} - 1 \end{matrix} \right\| \leq k_b^{k,t} + 1$$
$$p_{DC-loss_{conv}}^{k,t} = s^{k,t} c_{d0}^{k} + c_{d1}^{k} P_{abs}^{k,t} + c_{d2}^{k} k^{k,t}$$
$$p_{AC-loss_{conv}}^{k,t} = s^{k,t} c_{a0}^{k} + c_{a1}^{k} P_{abs}^{k,t} + c_{a2}^{k} k^{k,t}$$
$$P_{loss_b} = c_{b0}^{k} + c_{b1}^{k} k_b^{k,t}$$
$$SoC_{t+1}^{k} = SoC_t^{k} - \phi^{k} (p_b^{k,t} + p_{loss_b}^{k,t})$$
$$SoC_{t=1}^{k} = SoC_0^{k}$$
$$SoC_{t=T}^{k} = SoC_f^{k}$$
$$p_{bess}^{k,t} = p_b^{k,t} + p_{loss_b}^{k,t} + p_{DC-loss_{conv}}^{k,t}$$
$$p_{PV}^{k,t} = p_{pv}^{k,t} + p_{DC-loss_{conv}}^{k,t}$$
$$p_{WIND}^{k,t} = p_{wind}^{k,t} + p_{AC-loss_{conv}}^{k,t}$$
$$0 \leq SoC_t^{k} \leq 1$$
$$p_{min_b}^{k} \leq p_b^{k,t} \leq p_{max_b}^{k}$$
$$-p_{max_{DC-conv}}^{k} \leq p_{DC-loss_{conv}}^{k,t} \leq p_{max_{DC-conv}}^{k}$$
$$-p_{min_{gen}}^{k} \leq p_{gen}^{k,t} \leq p_{max_{gen}}^{k}$$
$$p_{min_{ren}}^{k} \leq p_{PV}^{k,t} \leq p_{max_{ren}}^{k}$$
$$p_{min_{ren}}^{k} \leq p_{WIND}^{k,t} \leq p_{max_{ren}}^{k}$$
$$-p_{max_{AC-conv}}^{k} \leq p_{AC-loss_{conv}}^{k,t} \leq p_{max_{AC-conv}}^{k}$$
$$u_{min} \leq u^{k,t} \leq u_{max}$$
$$-p_{max_l} \leq p_l^{s,t} \leq p_{max_l}$$
$$-p_{max_l} \leq p_l^{r,t} \leq p_{max_l} \tag{42}$$

The deterministic model (42) can be represented in compact form:

$$\min \; c^{\top} x + e^{\top} y \tag{43}$$

subject to

$$A_1 x = b_1 \tag{44}$$
$$A_2 x \leq b_2 \tag{45}$$
$$\|Fx\| \leq f^{\top} x \tag{46}$$
$$Hx + Ky = d \tag{47}$$
$$M_1 x = r_1 \tag{48}$$
$$M_2 x \leq r_2 \tag{49}$$
$$\|Gx\| \leq g^{\top} y, \tag{50}$$

where x and y are the vectors of decision variables for the first and second stages. Here, x corresponds to all energy management scheduling variables, while y corresponds to the power flow variables. The objective function (43) is separated into two stages in order to deal with the robust model more quickly in the next section. The first term of (43) represents the two first terms of the objective function of (42) ($f_{cost}^{device-losses}$ and f_{cost}^{gen}), while the second term of (43) represents the cost of grid losses in the objective function (42) ($f_{cost}^{grid-losses}$). Moreover, constraints (46) and (50) are the second-order cone inequalities for the first- and second-stage variables. Constraints (47) denote the nodal power balance equalities. Finally, (48) and (49) represent the linear equality and inequality constraints for the second-stage variables.

6) ROBUST ENERGY MANAGEMENT OPTIMIZATION MODEL

The demand and the primary sources of renewable energies are constantly changed during the DC-MG's operation. In addition, they have an inherent uncertainty that requires optimization methods such as stochastic programming [30], [31], [32], chance-constrained optimization [33], or robust optimization [34], [35]. Stochastic and chance-constrained

methods need a deep knowledge of the probability distribution function of the uncertain parameters to be applied, which is not always the case in real applications, since acquiring these data might not be possible. In contrast, when implementing robust optimization, the probability distribution functions of the uncertain parameters are not required. Moreover, robust optimization is computationally manageable and attractive [23], [36].

Now, the set that contains the demand and renewable generation uncertainty is defined as follows:

$$D^t(\bar{\mathbf{d}}^t, \hat{\mathbf{d}}^t) := \left\{ \begin{array}{c} \mathbf{d}^t \in \mathbf{R}^{|\Omega_n|} : d_k^t = \bar{d}_k^t + \hat{d}_k^t \left(\theta_+^{k,t} - \theta_-^{k,t}\right), \\ \theta_+^{k,t} + \theta_-^{k,t} \leq 1, \forall\, i \in \Omega_n \end{array} \right\}, \quad (51)$$

where $\theta_+^{k,t}$ and $\theta_+^{k,t}$ are binary variables employed to denote the uncertainty set; $\bar{d}_k^t$ is the power injected by renewable generation (or the required power demand); and $\hat{d}_k^t$ is the power deviation by renewable generation (or demand) from its nominal value.

In (51), it is possible to note that d_k^t can take the following value:

$$d_k^t \in [\bar{d}_k^t - \hat{d}_k^t,\ \bar{d}_k^t + \hat{d}_k^t]. \quad (52)$$

The proposed robust model is solved in two adaptive stages, as described in [22], which, in compact form, is as follows:

$$\begin{aligned} &\min_{\mathbf{x}} \left(\mathbf{c}^\top \mathbf{x} + \max_{\mathbf{d}\in D} \min_{\mathbf{y}\in\Omega(\mathbf{x},\mathbf{d})} \mathbf{e}^\top \mathbf{y} \right), \\ &\text{subject to} \\ &\quad \mathbf{A}_1\mathbf{x} = \mathbf{b}_1, \\ &\quad \mathbf{A}_2\mathbf{x} \leq \mathbf{b}_2, \\ &\quad \|\mathbf{F}\mathbf{x}\| \leq \mathbf{f}^\top \mathbf{x}, \end{aligned} \quad (53)$$

with

$$\Omega(\mathbf{x}, \mathbf{d}) = \left\{ \begin{array}{c} \mathbf{y} : \mathbf{H}\mathbf{x} + \mathbf{K}\mathbf{y} = \mathbf{d},\ \mathbf{M}_1\mathbf{x} = \mathbf{r}_1, \\ \mathbf{M}_2\mathbf{x} \leq \mathbf{r}_2,\ \|\mathbf{G}\mathbf{x}\| \leq \mathbf{g}^\top \mathbf{y}. \end{array} \right\} \quad (54)$$

Separating the robust energy management optimization model into two stages allows resolving the following. The first stage computes the variables associated with energy management optimization scheduling before the uncertainty is revealed. Even though the power flows are calculated in this stage, they do not represent their actual values, as they will be adjusted in the second stage, which includes the realization of uncertainty. Then, in order to determine the uncertainty, the first stage solves the energy management optimization again. All this shapes the two-stage, adaptive robust model proposed in [22].

IV. TEST SYSTEM AND RESULTS

A. ANALYZED SYSTEM

The proposed optimal energy management was evaluated in the modified IEEE 123-bus radial distribution feeder. This feeder was transformed into a single-phase equivalent, and the effects on the line reactances were neglected to obtain a DC test feeder. The location of the solar and wind generators and BESS were taken from [37], which considers seven solar power generators, ten wind power generators, and five BESS. The solar power generators are connected to nodes 19, 20, 37, 43, 50, 73, and 75, and the wind power generations are located at nodes 2, 4, 6, 47, 48, 85, 87, 107, 109, and 113. The BESS are connected to nodes 19, 33, 34, 64, and 75. Fig. 8 illustrates the modified IEEE 123 node test feeder, including the solar and wind power generators and the BESSs.

Figs. 5 and 6 present the available power to be delivered to each of these systems. These curves were obtained by employing information on wind speed, temperature, solar radiation, humidity, and pressure for periods of 0.5 h, which was taken from [38]. The demand variation throughout the day, the entirety of the renewable energy generators' available power, and the power purchasing costs are

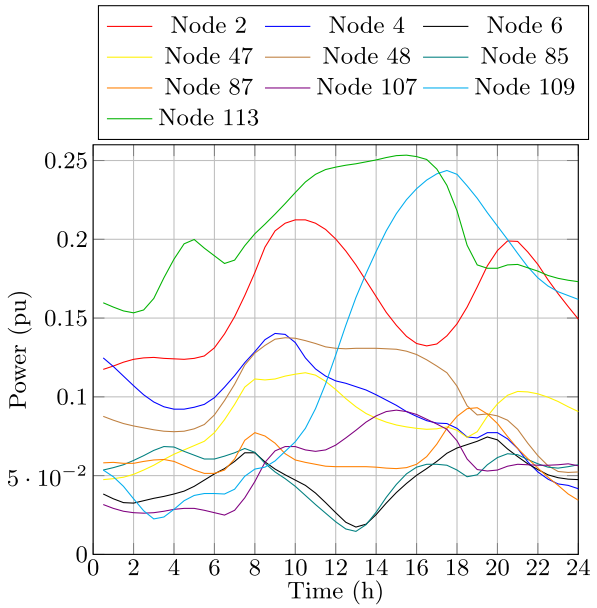

FIGURE 5. Available power for the wind generators.

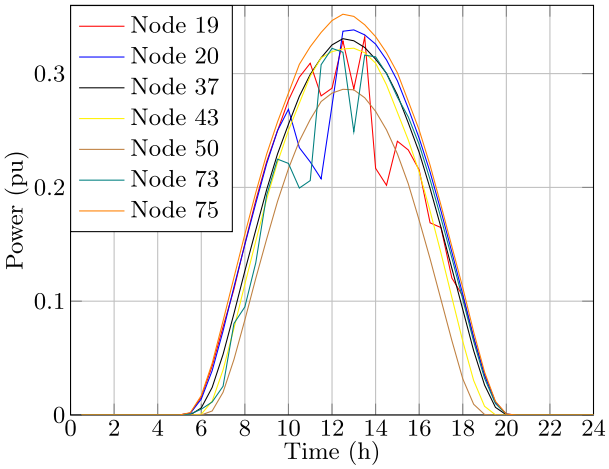

FIGURE 6. Available power for the PV generators.

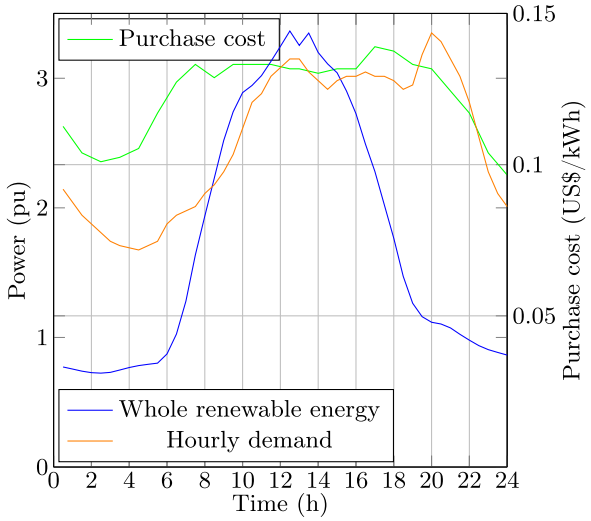

FIGURE 7. Energy purchasing cost (green line), hourly demand (orange line), and the entirety of the renewable energy generators' available power (blue line).

depicted in Fig 7. The peak purchase cost is assumed to be US$/kWh 0.1390.

B. RESULTS

The energy management mathematical model was implemented on a Dell Inspiron 15 7000 Series (Intel Quad-Core i7-7700HQ @2.80 GHz) personal computer, with 16 GB RAM and 64-bit Windows 10 Home Single Language, using the MATLAB 2021a software and the Yalmip toolbox [39], and it was optimized via the Gurobi solver [40].

Four scenarios were proposed to analyze the performance of the proposed convex model:

i. Scenario 1: Analysis of the deterministic model without considering uncertainties.
ii. Scenario 2: Analysis of energy management optimization while including demand uncertainty.
iii. Scenario 3: Analysis of energy management optimization while considering uncertainty in the solar and wind generators.
iv. Scenario 4: Analysis of the robust energy management optimization model, including uncertainty in the demand and solar and wind generators.

On the other hand, it was considered that the SoC of the BESS should be kept within 10-90%, according to experimental data presented in [41]. Furthermore, in two cases, the initial and final SoC of the BESSs were fixed to 50%, as recommended in [42].

1) DETERMINISTIC MODEL ANALYSIS

This subsection analyzes the optimal schedules generated by the proposed optimal model (42), which includes the power transfer losses in devices that interconnect renewable energies and BESS in the DC-MG. Note that the solution model (42) is defined as the deterministic solution, as it corresponds to the ideal formulation of the efficient operation of BESS and renewables in DC grids. This is due to the fact that it considers all external inputs (*i.e.*, demand behaviors and generation profiles) as data without any noise or uncertainty patterns. Under these simulated conditions, the expected daily operating costs of the IEEE 123-bus grid in its DC version are US$ 4376.82 per day.

Figs. 9a, 9b, and 9c present the total power dispatched by the generators, the power dispatched by the batteries, and their SoC, respectively. Based on these daily behaviors, it is noted that:

i. Fig. 9a shows the total power dispatched by the conventional, wind, and solar generators, as well as the total demand. The conventional generator is not required from 7:00 to 16:00, since the energy stored in the BESS plus the available renewable energy is more than the demand. From 8:00 to 13:00, renewable energy can supply the demand and charge the batteries, which allows reducing the system's operating costs.
ii. In addition, in Fig. 9a, it can be seen that the conventional generator is needed at times when the energy costs are higher. This is because the energy stored in the BESS is insufficient, or the BESSs are charging when the demand exceeds the distributed generators' availability (from 6:00 to 5:00 and at 16:00 hours).
iii. Figs. 9b and 9c show the behavior of the BESS during a day of operation, where it is confirmed that, when power generation is negative in these systems, they are storing energy. This implies that the SoC variable will increase. When the power injection in the BESS is positive, the BESS deliver energy, and the SoC variables decrease. Note, for example, that all batteries store energy from 00:00 to 5:00 and from 21:00 to 24:00. In addition, between 15:00 and 21:00, the BESS provide their stored energy to the grid in order to compensate for the significant reduction in power generation by PV sources, thus contributing to reduce the amount of power generated in the conventional source and aid in daily operating costs minimization.
iv. The critical behavior of the BESS goes from 5:00 to 15:00 hours. During this period, these devices store energy due to the energy surpluses from renewables, to later return it when the total demand behavior increases, with the aim to contribute to local energy loss reduction in the vicinity of the batteries' connection. In addition, the BESSs store energy from 9:00 to 15:00 in order to deliver it when PV availability is reduced during the afternoon and night.

2) OPTIMAL ENERGY MANAGEMENT WHILE INCLUDING DEMAND UNCERTAINTY

This section analyzes the optimal schedules generated while considering demand uncertainty in the proposed optimal model (53). This scenario considers a demand uncertainty of $\pm$ 5% of the nominal value. According to [43], this value was assumed because the prediction error of demand loads with

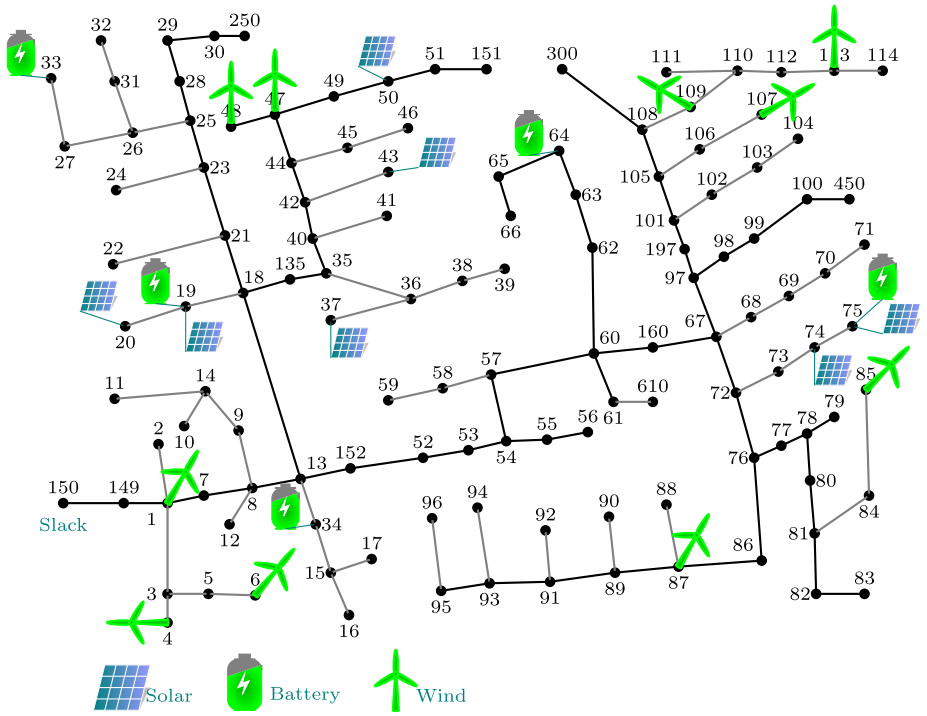

FIGURE 8. Modified 123-IEEE DC test system.

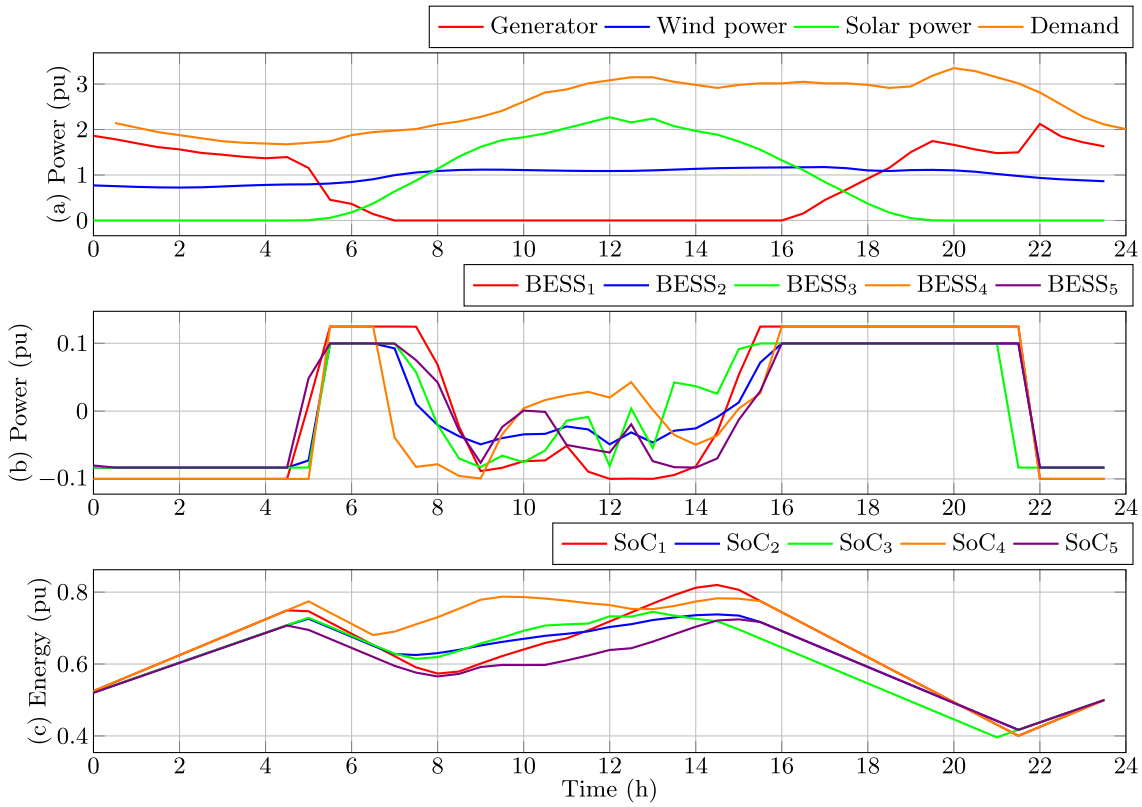

FIGURE 9. Results for scenario 1: (a) total power dispatched by the generators and demand, (b) power dispatched by the BESS, and (c) SoC of the BESS.

maximum generation was around 5%. Fig. 10 illustrates the demand variation considered in this paper.

In this scenario, the operating costs are US$ 5243.23, which is an increase of 19.79% compared to scenario 1.

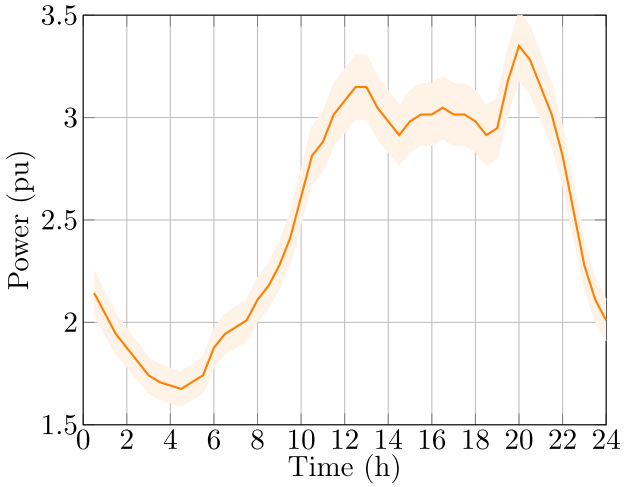

FIGURE 10. Demand with the uncertainty – ± 5% of the nominal value.

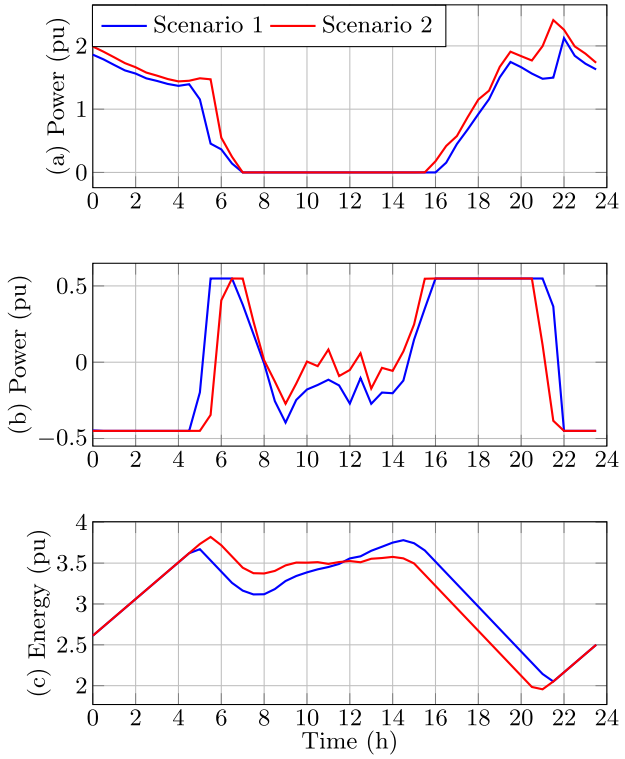

FIGURE 11. Results for scenario 2: (a) total power dispatched by the conventional generators, (b) Total power dispatched by the BESS, and (c) total SoC of the BESS.

This increase is expected, as the proposed optimal energy management schedules the generators in a worse scenario.

Fig. 11a presents the total power dispatched by the conventional generator for scenarios 1 and 2. Note that this power increases from 00:00 to 7:00 and from 15:00 to 24:00 regarding scenario 1 in order to satisfy demand uncertainty. At the same time, the total power dispatched by the conventional generator is still not required from 7:00 to 16:00. This is due to two facts: first, the dispatched powers of the solar and wind generators have not changed; secondly, the battery charge and discharge schedules have changed (Figs. 11b and 11c) to

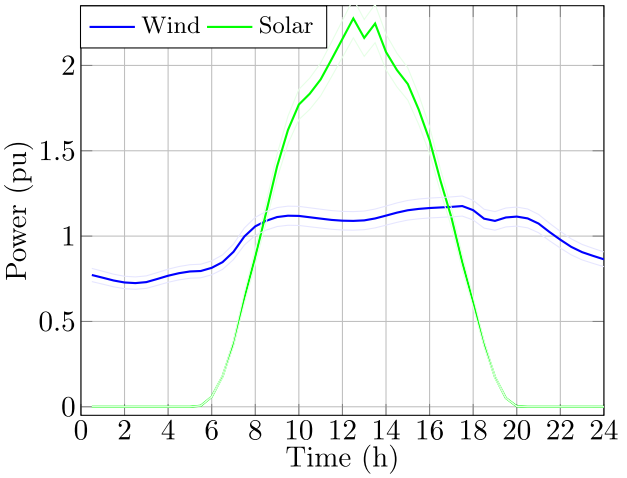

FIGURE 12. Total power available of the solar and wind generators with ± 5% uncertainties in their nominal value.

prepare for the worst possible scenario concerning demand uncertainty.

As seen in Figs. 11b and 11c, the total scheduled power of the BESS starts being delivered to the system one hour later than in scenario 1 (5:00 hours). Meanwhile, the BESS has been charging for an hour longer than scenario 1, which allows for delivering more energy from 15:00 to 21:00– during this period, the available solar energy drastically drops.

3) OPTIMAL ENERGY MANAGEMENT WHILE INCLUDING UNCERTAINTY IN SOLAR AND WIND GENERATORS

This section analyzes the optimal schedules generated while only considering uncertainty in the solar and wind generators. This scenario only includes ± 5% uncertainties in the nominal values for the solar and wind generators. This range was considered [44] since a typical prediction error of 5% regarding renewable energies with maximum generation has been observed. Fig. 12 depicts the total power available for the solar and wind generators, including their uncertainties.

In this scenario, the operating costs are US$ 5072.23, which constitutes an increase of 15.88% compared to scenario 1. Similar to scenario 2, the operating costs are higher than those of scenario 1. This result is expected, given that the generators are programmed for the worst-case scenario. Additionally, the operating costs are less than those of scenario 2. This indicates that the effect of demand uncertainty has greater weight in the programming of the entire DC-MG.

Figs. 13a, 13b, and 13c show the total power dispatched by the conventional generator and batteries, as well as the total battery SoC for scenarios 3 and 1.

Fig. 13a illustrates the total power dispatched by the conventional generator for scenarios 1 and 3. Note that it increases from 00:00 to 7:00 and from 15:00 to 24:00 in scenario 1. This is to satisfy demand uncertainty. Here, the conventional generator dispatches power from 7:00 to 16:00 hours, which did not occur in the two previous scenarios. This is because solar and wind power have the most

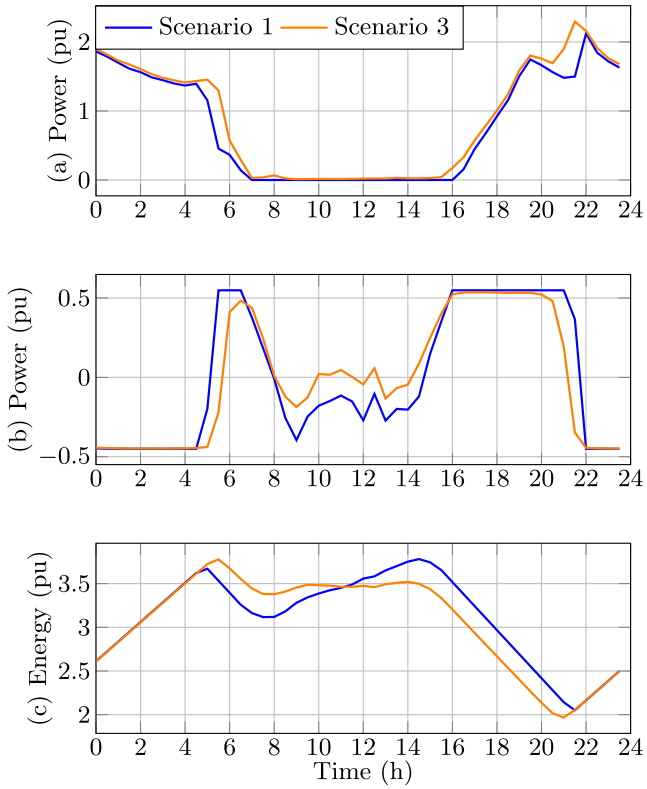

FIGURE 13. Results for scenario 3: (a) total power dispatched by the conventional generator, (b) total power dispatched by the BESS, and (c) total SoC of the BESS.

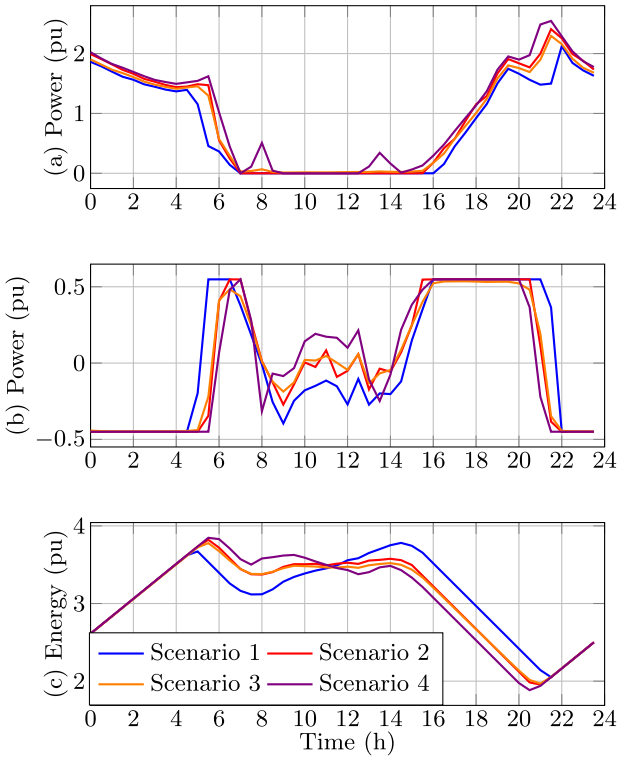

FIGURE 14. Results for scenario 4: (a) total power dispatched by the conventional generator, (b) total power dispatched by the, and (c) total SoC of the BESS.

significant impact on the available energy. Hence, a great uncertainty, whereby the conventional generator may be required, increases the operating costs of the microgrid.

Fig. 13b shows that the total scheduled power in the BESS is delivered to the system one hour later than in scenario 1 (5:00 hours). Furthermore, the power absorbed by the batteries in the period from 8:00 to 15:00 hours is less than that in scenario 1. In turn, Fig. 13c reveals that the total BESS SoC is charged for an hour longer at startup than in scenario 1, alleviating the uncertainty of the renewable energies.

4) OPTIMAL ENERGY MANAGEMENT WHILE INCLUDING UNCERTAINTY IN DEMAND AND THE SOLAR AND WIND GENERATORS

This scenario analyzes the robust optimal schedules generated by the proposed optimal model (53) while including uncertainty in demand and in the solar and wind generators. This scenario includes uncertainties in demand and solar and wind generators, and these uncertainties are illustrated in Figs. 10 and 12.

The operating cost is US$ 5738.75, which is the highest among the studied scenarios. This value exceeds the others by 31.12%, 9.45%, and 13.14% with respect to scenarios 1, 2, and 3. This result is logical since, in scenario 4, there is a more significant uncertainty. Hence, the generators are scheduled in the face of the worst-case scenario.

Figs. 14a, 14b, and 14c show the total dispatched power of the conventional generator and the batteries, as well as the total battery SoC for all scenarios.

The total power dispatched by the conventional generator for all scenarios is shown in Fig. 14a. As expected, for scenario 4, this generator is scheduled and dispatched for more time and power than in other scenarios. This behavior is logical, as scenario 4 involves a more significant uncertainty that must be supplied. According to Fig. 14a, at 8:00 and 15:00 hours, the conventional generator is required to a greater extent in scenario 4.

By analyzing Fig. 14b, note that the total scheduled power absorbed by the BESS in the DC-MG is maintained for a longer time in scenario 4 (until 7:00 hours). In addition, from 9:00 to 13:00, the BESSs deliver greater power in scenario 4 than in the other scenarios, with the aim of compensating for the considered uncertainties.

The total BESS SoC in Fig. 14c shows that scenario 4 involves charging for a longer time at startup than in other scenarios, thus allowing to compensate in other periods, especially when there is a more significant uncertainty in the DC-MG.

V. CONCLUSION

This paper proposed a robust optimal energy management model for BESS and renewable energies in DC microgrids via a convex formulation. This formulation ensured the global optimum of the problem, even when considering uncertainty

since it is minimized regarding the worst-case cost while satisfying all of its constraints. Additionally, the power transfer losses in power converter devices were included and convexified in a robust energy management model. This convexification was performed by transforming the non-linear non-convex equations into second-order cone constraints. Four scenarios were proposed to analyze the model: the deterministic model, demand uncertainty, uncertainty in the solar and wind generators, and uncertainty in demand and solar and wind generators. In all four scenarios, the goal was to reduce the total energy costs, including the costs of power transfer and network losses, as well as the cost of energy. Scenario 4 reported the highest costs of the problem, given that, in this scenario, there was more uncertainty involved, and the optimal robust energy management model dispatched more energy from the conventional generator, thus increasing the operating costs to be able to program all BESS and renewable energies for the worst-case cost. The operating costs, with respect to scenario 4, increased by 31.12%, 9.45%, and 13.14% for scenarios 1, 2, and 3, respectively.

The following works could be conducted in the future: (i) extending the proposed model to bipolar DC microgrids with asymmetrical loads, as well as to AC networks with single- and three-phase topologies; (ii) including an objective function regarding the minimization of the total CO_2 emissions by conventional sources (substations and diesel sources) in the proposed convex model; and (iii) modifying the proposed convex formulation to include monopolar DC networks with meshed topologies.

REFERENCES

[1] D. R. Raimundo, I. F. S. D. Santos, G. L. T. Filho, and R. M. Barros, "Evaluation of greenhouse gas emissions avoided by wind generation in the Brazilian energetic matrix: A retroactive analysis and future potential," *Resour., Conservation Recycling*, vol. 137, pp. 270–280, Oct. 2018.

[2] M. A. Hajer and P. Pelzer, "2050—An Energetic Odyssey: Understanding 'techniques of futuring' in the transition towards renewable energy," *Energy Res. Social Sci.*, vol. 44, pp. 222–231, Oct. 2018.

[3] R. Li, W. Wang, and M. Xia, "Cooperative planning of active distribution system with renewable energy sources and energy storage systems," *IEEE Access*, vol. 6, pp. 5916–5926, 2018.

[4] X. Yang and F. Xiao, "Research on voltage control of multi terminal flexible medium voltage DC distribution network," *J. Phys., Conf. Ser.*, vol. 1639, no. 1, Oct. 2020, Art. no. 012052.

[5] Y. Fan, Y. Chi, Y. Li, Z. Wang, H. Liu, W. Liu, and X. Li, "Key technologies for medium and low voltage DC distribution system," *Global Energy Interconnection*, vol. 4, no. 1, pp. 91–103, Feb. 2021.

[6] T. Dragičević, X. Lu, J. C. Vasquez, and J. M. Guerrero, "DC microgrids—Part II: A review of power architectures, applications, and standardization issues," *IEEE Trans. Power Electron.*, vol. 31, no. 5, pp. 3528–3549, May 2016.

[7] O. D. Montoya, W. Gil-González, L. Grisales-Noreña, C. Orozco-Henao, and F. Serra, "Economic dispatch of BESS and renewable generators in DC microgrids using voltage-dependent load models," *Energies*, vol. 12, no. 23, p. 4494, Nov. 2019.

[8] D. Zarrilli, A. Giannitrapani, S. Paoletti, and A. Vicino, "Energy storage operation for voltage control in distribution networks: A receding horizon approach," *IEEE Trans. Control Syst. Technol.*, vol. 26, no. 2, pp. 599–609, Mar. 2018.

[9] Z. Wang, H. Lin, and Y. Ma, "A control strategy of modular multilevel converter with integrated battery energy storage system based on battery side capacitor voltage control," *Energies*, vol. 12, no. 11, p. 2151, Jun. 2019.

[10] X. Li and S. Wang, "Energy management and operational control methods for grid battery energy storage systems," *CSEE J. Power Energy Syst.*, vol. 7, no. 5, pp. 1026–1040, 2021.

[11] M. Zidar, P. S. Georgilakis, N. D. Hatziargyriou, T. Capuder, and D. Škrlec, "Review of energy storage allocation in power distribution networks: Applications, methods and future research," *IET Generat., Transmiss. Distrib.*, vol. 10, no. 3, pp. 645–652, Mar. 2016.

[12] A. W. Bizuayehu, A. A. S. de la Nieta, J. Contreras, and J. P. S. Catalão, "Impacts of stochastic wind power and storage participation on economic dispatch in distribution systems," *IEEE Trans. Sustain. Energy*, vol. 7, no. 3, pp. 1336–1345, Jul. 2016.

[13] X. Shen, M. Shahidehpour, Y. Han, S. Zhu, and J. Zheng, "Expansion planning of active distribution networks with centralized and distributed energy storage systems," *IEEE Trans. Sustain. Energy*, vol. 8, no. 1, pp. 126–134, Jan. 2017.

[14] A. F. Peñaranda, D. Romero-Quete, and C. A. Cortés, "Grid-scale battery energy storage for arbitrage purposes: A Colombian case," *Batteries*, vol. 7, no. 3, p. 59, Sep. 2021.

[15] A. Valencia, R. A. Hincapie, and R. A. Gallego, "Optimal location, selection, and operation of battery energy storage systems and renewable distributed generation in medium–low voltage distribution networks," *J. Energy Storage*, vol. 34, Feb. 2021, Art. no. 102158.

[16] W. Gil-González, O. D. Montoya, E. Holguín, A. Garces, and L. F. Grisales-Noreña, "Economic dispatch of energy storage systems in DC microgrids employing a semidefinite programming model," *J. Energy Storage*, vol. 21, pp. 1–8, Feb. 2019.

[17] A. Soroudi, *Power System Optimization Modeling in GAMS*. Cham, Switzerland: Springer, 2017.

[18] L. Novoa, R. Flores, and J. Brouwer, "Optimal renewable generation and battery storage sizing and siting considering local transformer limits," *Appl. Energy*, vol. 256, Dec. 2019, Art. no. 113926.

[19] L. F. Grisales-Noreña, O. D. Montoya, and C. A. Ramos-Paja, "An energy management system for optimal operation of BSS in DC distributed generation environments based on a parallel PSO algorithm," *J. Energy Storage*, vol. 29, Jun. 2020, Art. no. 101488.

[20] L. F. Grisales-Noreña, O. D. Montoya, and J. C. Hernández, "An efficient EMS for BESS in monopolar DC networks with high penetration of renewable generation: A convex approximation," *Batteries*, vol. 9, no. 2, p. 84, Jan. 2023.

[21] H. Shafique, L. B. Tjernberg, D.-E. Archer, and S. Wingstedt, "Energy management system (EMS) of battery energy storage system (BESS)—providing ancillary services," in *Proc. IEEE Madrid PowerTech*, Jun. 2021, pp. 1–6.

[22] B. Zeng and L. Zhao, "Solving two-stage robust optimization problems using a column-and-constraint generation method," *Oper. Res. Lett.*, vol. 41, no. 5, pp. 457–461, 2013.

[23] I. Sarantakos, M. Peker, N.-M. Zografou-Barredo, M. Deakin, C. Patsios, T. Sayfutdinov, P. C. Taylor, and D. Greenwood, "A robust mixed-integer convex model for optimal scheduling of integrated energy storage—Soft open point devices," *IEEE Trans. Smart Grid*, vol. 13, no. 5, pp. 4072–4087, Sep. 2022.

[24] H. Akagi, T. Yamagishi, N. M. L. Tan, S. Kinouchi, Y. Miyazaki, and M. Koyama, "Power-loss breakdown of a 750-V 100-kW 20-kHz bidirectional isolated DC–DC converter using SiC-MOSFET/SBD dual modules," *IEEE Trans. Ind. Appl.*, vol. 51, no. 1, pp. 420–428, Jan. 2015.

[25] C. Patsios, B. Wu, E. Chatzinikolaou, D. J. Rogers, N. Wade, N. P. Brandon, and P. Taylor, "An integrated approach for the analysis and control of grid connected energy storage systems," *J. Energy Storage*, vol. 5, pp. 48–61, Feb. 2016.

[26] *Power Losses in Voltage Sourced Converter (VSC) Valves for High-Voltage Direct Current (HVDC) Systems*, Standard BS EN 62751-1:2014+A1, British Standards Institution, Tech. Rep., Jun. 2018. [Online]. Available: https://standards.iteh.ai/catalog/standards/clc/7fe9e5ce-ad04-4661-aac4-9dd64685905c/en-62751-1-2014-a1-2018

[27] M. H. Bierhoff and F. W. Fuchs, "Semiconductor losses in voltage source and current source IGBT converters based on analytical derivation," in *Proc. IEEE 35th Annu. Power Electron. Spec. Conf.*, Jun. 2004, pp. 2836–2842.

[28] F. M. Gatta, A. Geri, S. Lauria, M. Maccioni, and F. Palone, "Battery energy storage efficiency calculation including auxiliary losses: Technology comparison and operating strategies," in *Proc. IEEE Eindhoven PowerTech*, Jul. 2015, pp. 1–6.

[29] *IEEE Guide for Optimizing the Performance and Life of Lead-Acid Batteries in Remote Hybrid Power Systems*, Standard 1561–2019 (Revision IEEE Std 1561–2007), 2019, pp. 1–34.
[30] M. Peker, A. S. Kocaman, and B. Y. Kara, "A two-stage stochastic programming approach for reliability constrained power system expansion planning," *Int. J. Electr. Power Energy Syst.*, vol. 103, pp. 458–469, Dec. 2018.
[31] M. Peker, A. S. Kocaman, and B. Y. Kara, "Benefits of transmission switching and energy storage in power systems with high renewable energy penetration," *Appl. Energy*, vol. 228, pp. 1182–1197, Oct. 2018.
[32] J. Wang, N. Zhou, and Q. Wang, "Data-driven stochastic service restoration in unbalanced active distribution networks with multi-terminal soft open points," *Int. J. Electr. Power Energy Syst.*, vol. 121, Oct. 2020, Art. no. 106069.
[33] D. Huo, C. Gu, D. Greenwood, Z. Wang, P. Zhao, and J. Li, "Chance-constrained optimization for integrated local energy systems operation considering correlated wind generation," *Int. J. Electr. Power Energy Syst.*, vol. 132, Nov. 2021, Art. no. 107153.
[34] H. Ji, C. Wang, P. Li, F. Ding, and J. Wu, "Robust operation of soft open points in active distribution networks with high penetration of photovoltaic integration," *IEEE Trans. Sustain. Energy*, vol. 10, no. 1, pp. 280–289, Jan. 2019.
[35] D. Bertsimas, E. Litvinov, X. A. Sun, J. Zhao, and T. Zheng, "Adaptive robust optimization for the security constrained unit commitment problem," *IEEE Trans. Power Syst.*, vol. 28, no. 1, pp. 52–63, Feb. 2013.
[36] A. Gholami, T. Shekari, and S. Grijalva, "Proactive management of microgrids for resiliency enhancement: An adaptive robust approach," *IEEE Trans. Sustain. Energy*, vol. 10, no. 1, pp. 470–480, Jan. 2017.
[37] D.-A. Ramirez, A. Garcés, and J.-J. Mora-Flórez, "A convex approximation for the tertiary control of unbalanced microgrids," *Electr. Power Syst. Res.*, vol. 199, Oct. 2021, Art. no. 107423.
[38] SoDa Solar Radiation Data. *Solar Training*. Accessed: Mar. 28, 2022. [Online]. Available: https://www.soda-pro.com
[39] J. Lofberg, "YALMIP : A toolbox for modeling and optimization in MATLAB," in *Proc. IEEE Int. Conf. Robot. Autom.*, Sep. 2004, pp. 284–289.
[40] Gurobi Optimization, LLC. (2022). *Gurobi Optimizer Reference Manual*. Accessed: Nov. 22, 2022. [Online]. Available: https://www.gurobi.com
[41] M. S. H. Lipu, M. A. Hannan, A. Hussain, A. Ayob, M. H. M. Saad, and K. M. Muttaqi, "State of charge estimation in lithium-ion batteries: A neural network optimization approach," *Electronics*, vol. 9, no. 9, p. 1546, Sep. 2020.
[42] O. D. Montoya, A. Grajales, A. Garces, and C. A. Castro, "Distribution systems operation considering energy storage devices and distributed generation," *IEEE Latin Amer. Trans.*, vol. 15, no. 5, pp. 890–900, May 2017.
[43] Y. Chen and H. Tan, "Short-term prediction of electric demand in building sector via hybrid support vector regression," *Appl. Energy*, vol. 204, pp. 1363–1374, Oct. 2017.
[44] G.-Q. Lin, L.-L. Li, M.-L. Tseng, H.-M. Liu, D.-D. Yuan, and R. R. Tan, "An improved moth-flame optimization algorithm for support vector machine prediction of photovoltaic power generation," *J. Cleaner Prod.*, vol. 253, Apr. 2020, Art. no. 119966.

WALTER GIL-GONZÁLEZ (Member, IEEE) was born in Pereira, Colombia, in 1986. He received the B.Sc., M.Sc., and Ph.D. degrees in electrical engineering from Universidad Tecnológica de Pereira, Colombia, in 2011, 2013, and 2019, respectively. He was an Adjunct Professor with Institución Universitaria Pascual Bravo. He is currently an Assistant Professor with the Department of Electric Power Engineering, Universidad Tecnológica de Pereira. His research interests include power systems control and stability and the optimization and operation of electrical distribution systems.

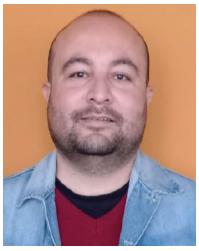

OSCAR DANILO MONTOYA (Member, IEEE) was born in Obando, Valle, Colombia, in 1989. He received the B.E.E., M.Sc., and Ph.D. degrees in electrical engineering from Universidad Tecnológica de Pereira, Colombia, in 2012, 2014, and 2019, respectively. He is currently an Assistant Professor with the Electrical Engineering Program, Universidad Distrital Francisco José de Caldas, Colombia. His research interests include mathematical optimization, planning and control of power systems, renewable energies, energy storage, protective devices, passivity-based control, and dynamical analysis.

JESÚS C. HERNÁNDEZ was born in Jaén, Spain. He received the M.Sc. and Ph.D. degrees from the University of Jaén, in 1994 and 2003, respectively. Since 1995, he has been an Associate Professor with the Department of Electrical Engineering, University of Jaén. His current research interests include smart grids, smart meters, renewable energy, and power electronics.